Chinese Chemical Letters 34 (2023) 108357

Contents lists available at ScienceDirect

Chinese Chemical Letters

journal homepage: www.elsevier.com/locate/cclet

Iron-based biochar as efficient persulfate activation catalyst for emerging pollutants removal: A review

Jinjie Lu[a], Qinwei Lu[a], Lu Di[a], Yi Zhou[a], Yanbo Zhou[a,b,*]

[a] State Environmental Protection Key Laboratory of Environmental Risk Assessment and Control on Chemical Process, East China University of Science and Technology, Shanghai 200237, China
[b] School of Carbon Neutrality Future Technology, East China University of Science and Technology, Shanghai 200237, China

ARTICLE INFO

Article history:
Received 21 November 2022
Revised 16 March 2023
Accepted 20 March 2023
Available online 22 March 2023

Keywords:
Biochar
Persulfate
Emerging pollutants

ABSTRACT

In recent years, biochar (BC) as a low-cost, easily available biomass product, is widely applied in sulfate radical-based advanced oxidation processes (SR-AOPs) for emerging pollutants remediation. Herein, a state-of-art review of iron-based biochar catalysts is currently available in SR-AOPs application. A general summary of the development of biochar and the catalytic properties of biochar is presented. Especially, the synthetic strategies of different types of iron-based biochar catalysts are discussed. Moreover, the theoretical calculation to interpret the interaction between biochar and iron species is discussed to explore the activation mechanisms. And the regeneration methods of biochar-based catalyst are presented. The unresolved challenges of the existent biochar-based SR-AOPs are pointed out, and the outlooks of future research directions are proposed.

1. Introduction

To date, emerging pollutants such as organic pesticides, pharmaceuticals and personal care products (PPCPs), and endocrine disrupting chemicals (EDCs) have raised wide concern due to high toxicity, persistence, and bio-accumulation [1,2]. Emerging pollutants come from several sources such as industrial wastewater, and municipal wastewater, thus posing threat to human and ecosystem safety [3–6]. Different from traditional pollutants, the concertation of emerging pollutants is commonly at a low level, even reaching to trace concertation level, which means traditional water treatment methods are hard to deal with them [7–9].

Advanced oxidation processes (AOPs) provide a powerful capacity of degrading and even mineralizing emerging pollutants through reactive oxygen species (ROS) [10]. According to different oxidants, AOPs can be divided into Fenton oxidation, photocatalysis, potassium permanganate oxidation, and persulfate oxidation. Among them, sulfate-based advanced oxidation processes (SR-AOPs) have attracted much attention in recent years. And the main advantages of SR-AOPs are as follows: (1) solid persulfate transport is safer than common oxidants liquid H_2O_2; (2) high redox potential ($E^0(SO_4^{\bullet-}/SO_4^{2-}) = 2.6\text{-}3.1$ V) could bring strong oxidation ability; (3) wide pH range (pH 2-9) has more wide application scenarios [11,12]; (4) shorter distance of O-O bond (HSO_5^- and H_2O_2 are 1.453 and 1.460 Å, respectively) [13]; (5) lower bond energy (in the range of 140–213.3 kJ/mol) [12].

The SR-AOPs research mainly focused on the high efficiency of persulfate activation. Various activation methods have been researched, including UV, heat [14], transition metals [15–17], and carbon materials [18–21]. Anipsitakis *et al.* studied the degradation of 2,4-dichlorophenol by different transition metal activated PMS. And they found the degradation efficiency was as follows: $Co^{2+} > Fe^{2+} > Ce^{3+} > V^{3+} > Mn^{2+} > Fe^{3+}$ [22]. Since then, many researchers developed heterogeneous transition metal catalysts to overcome homogeneous catalysts may bring secondary pollution. Transition metal catalysts exhibit extremely high catalytic activity, but they will also face the defects of nanoparticle agglomeration and metal leaching. Carbonaceous materials with superior catalysis performance, which can avoid metal leaching, are now widely used in persulfate activation [23]. In 2012, Sun *et al.* found that reduced graphene oxide (rGO) has better activation ability than typical cobalt-based catalysts Co_3O_4 [18]. The removal efficiency of phenol by rGO and Co_3O_4 was 70.4% and 23.9%, respectively. Similar experimental results were obtained for the degradation of DCP and MB, which set off a boom in the research of catalytic persulfate by carbon materials. Researchers have found that activated carbon (AC), carbon nanotubes (CNTs), nanodiamonds (ND), and graphene (GO) also have catalytic abilities [24,25]. For example, Zhang *et al.* found that PMS was directly activated by granular

* Corresponding author at: State Environmental Protection Key Laboratory of Environmental Risk Assessment and Control on Chemical Process, East China University of Science and Technology, Shanghai 200237, China.
E-mail address: zhouyanbo@ecust.edu.cn (Y. Zhou).

https://doi.org/10.1016/j.cclet.2023.108357
1001-8417/

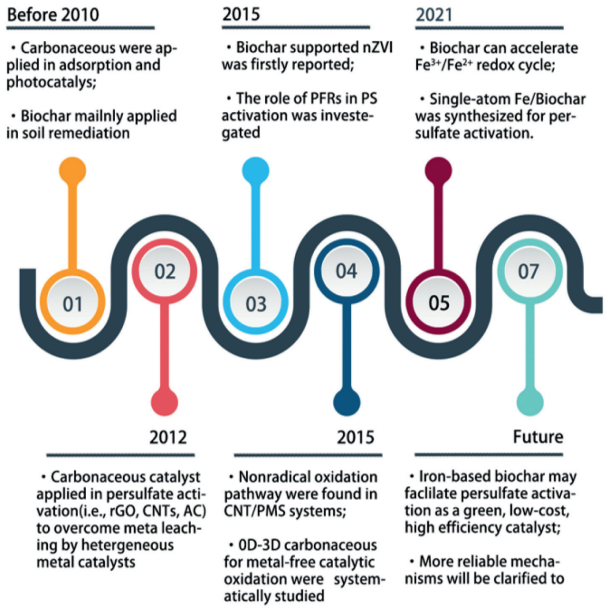

Fig. 1. Timeline exhibiting the breakthrough in the development of biochar catalysts applied in environmental field.

activated carbon, and there was no significant decline after four times recycling [26]. Duan *et al.* investigated 0D-3D carbonaceous materials and found that the dimensionality and surface chemistry of carbonaceous materials determine the catalytic activity, and 3D carbonaceous materials are superior to low-dimensional carbon materials in both adsorption and catalytic performance [27]. What is more, Lee found that methanol quenching could not inhibit the activation of persulfate by CNTs, which means existing non-radical pathways direct electron transfer during the antibiotics degradation process [28]. To further improve the metal-free carbonaceous catalyst performance, researchers doped heteroatom and loaded metal nanoparticles on carbonaceous materials to modulate the local carbon layer charge. Wang constructed Fe_3C@NCNT to achieve complete degradation of phenol within 20 min, and the encapsulated Fe_3C nanoparticles played a good synergistic effect with the outer carbon [29].

The excellent performance of carbonaceous materials has been well demonstrated, but carbonaceous catalysts such as graphene and carbon nanotubes suffer from complicated preparation procedures, high production costs, and insufficient durability, which limit large-scale applications. Biochar has abundant oxygen functional groups on the surface, which offers them excellent potential in adsorption and catalysis.

Biochar materials were mainly applied in pollutants adsorption in soil and wastewater. Researchers often focused on the effects of biomass feedstock and pyrolysis conditions on adsorption capacity. To fulfill its goal of carbon neutrality, in recent years biochar has more wide applications in catalysis, battery [30], and bio-oil [31]. In the database of Web of Science, the number of papers on the topic of 'biochar' has increased steadily in Fig. S1 (Supporting information), showing the trend of biochar becoming gradually hot. Among them, the number of publications that applied biochar to persulfate activation shows an increasing tendency in the past three years, which have made outstanding contributions to the scientific research of the environment (Fig. 1).

In this review, we will start by introducing the basic structure of biochar, which may influence the performance of persulfate activation, mainly focused on biomass feedstock and pyrolysis conditions. Different modification methods are also discussed. What is more, iron-loaded biochar is a hot research issue, but still lacks a review focus on the interaction between iron and biochar. The challenges and prospects of the application of biochar catalysts, such as regeneration methods, application scenario, and future research direction are also discussed. This review aims to present state-of-art knowledge of biochar catalysts to reduce the future risk of emerging pollutants.

2. Biochar structure affected catalysis performance

Biochar is the pyrolysis product of biomass under an oxygen-limited atmosphere. Theoretically, all organic biomass can be used as feedstock for the preparation of biochar. The raw materials could be founded from a variety of sources. The preparation method is simple, and waste recycling can be realized. Therefore, the application of biochar for persulfate activation will be a win-win strategy [32,33].

Biochar comprises four basic elements, C, H, O, and N. Compared to activated carbon, a variety of inorganic elements such as Si, K, and Ca are present in biochar [34,35]. The mineral elements may block the micropore in the carbon matrix, resulting in relatively low specific surface area in biochar. Pyrolysis of different biomass feedstocks will result in remarkable differences. The content of each element mainly depends on the biomass feedstock. Also, the performance of persulfate activation is largely influenced by biomass feedstock, which can be classified into three categories: plant-derived biomass, animal remains-derived biomass, and sludge-derived biomass [36].

The main components in plant-derived biomass are cellulose, hemicellulose, and lignin. It also can be called lignocellulosic biochar. With the increase in pyrolysis temperature, the carbon layer structure will transform from amorphous aromatic carbon to conjugated aromatic carbon and then to graphite-type carbon [37]. At the same time, the specific surface area of biochar tends to increase, which is related to adsorption capacity, facilitating surface interaction with containment molecules [38]. Compared to plant-derived biochar, sludge-derived biochar tends to exhibit stronger catalytic ability due to the widely used flocculants such as polyacrylamide, polymerized ferric sulfate, and polymerized aluminum chloride in wastewater treatment, which makes it easier to achieve the nitrogen-doped and iron-loaded on biochar. Also, due to the high ash content of sludge biochar, etching and structural modulation by strong acids (such as HF and HNO_3) are often required to expose more active sites. But using strong acid etching may increase the preparation cost and environmental risk. Therefore, researchers nowadays mainly focus on plant-derived biochar. At the same time, the rational utilization of sludge-derived biochar will remain one of the priorities of future researchers, which will greatly ease the pressure of sludge disposal and reduce treatment costs.

Usually, the specific surface area (SSA) of biochar tends to increase gradually with pyrolysis temperature increasing. However, compared with conventional activated carbon, the SSA of pristine biochar is still relatively small, usually below 150 m^2/g [39]. Therefore, the low SSA limits biochar performance in adsorption and catalysis, and often requires activation to enlarge the pore channels and increase the specific surface area, such as chemical activation (NaOH, KOH), and steam activation (CO_2, H_2O). Compared with N_2 and CO_2, Sun *et al.* found that CO_2 better created the multistage pore structure while improving the graphitization of biochar [40]. The researchers found that the specific surface area of biochar modified with iron-based materials also increased [41]. The presence of iron in biomass precursors can alter the distribution of pyrolysis products as well as the biochar properties, inhibit tar formation, and promote the enlargement of pore structure [42]. And iron carbide mediates oxidation of carbon matrix at a higher temperature which increases specific surface area and fuses

micropores to form mesopores [43,44]. The enlargement of the specific surface area can increase the potential adsorption capacity [45].

In addition to elemental composition and specific surface area, persistent free radicals (PFRs) are important surface functional components. They are in form of carbon or oxygen-centered unpaired electrons forming resonance-stabilized structures of radicals through self-destruct, such as semiquinone radicals and phenoxy radicals are considered typical representatives of oxygen-centered radicals. PFRs are mainly present in biochar pyrolyzed at low temperatures. In general, PFRs could be further decayed as pyrolysis temperature and time continued to increase [46]. Yet, if the pyrolysis temperature exceeds 700 °C, the PFRs will decompose rapidly due to the breakdown and reorganization of organic structures [47]. The formation mechanisms of PFRs and the affecting factors on the concentrations and types of PFRs in biochar are still not fully elucidated owing to the highly variable synthesis methods, diverse precursors, and complex reaction processes. Different pyrolysis temperature and time will have a synergy effect on PFRs concentrations. Not only synthesis may influent the PFRs concentrations, but also external metal loaded on biochar can change the type and concentration of PFRs in biochar. Fang *et al.* found that the concentration and structure of PFRs could be directionally manipulated by appropriate loading of transition metals (Fe^{3+}, Cu^{2+}, Ni^{2+}, and Zn^{2+}) and phenolic compounds (*p*-diphenol, phenol) at low concentration [48,49]. Ruan *et al.* explored the process of lignin pyrolysis and found that the addition of $FeCl_3$ promoted dehydration and deacidification to generate PFRs chelated with iron ions [46,50]. And their concentration increased from 0.0371 mmol/g to 0.0655 mmol/g, and the BPA degradation efficiency increased from 60% to 80%. Hence, the construction of iron-based biochar catalysts can introduce more active sites including PFRs and iron sites.

3. Modification of biochar

Pristine biochar still faces the shortcomings of low specific surface area and unstable catalysis performance limiting its practical application. To overcome these intrinsic shortcomings, introducing iron species and doping heteroatoms to improve activity might be the optimal strategy for designing efficient and stable biochar-based catalysts [51]. In this section, common synthesis methods of iron-based biochar catalysts and application performance are summarized. The catalysis performance of different modified biochar catalysts is shown in Table S1 (Supporting information). In short, pretreating biomass using iron salt before pyrolysis is facile and cheap, and the properties of obtained catalysts are easily controlled by synthesis parameters, which may benefit future large-scale catalyst production.

3.1. Nano-ZVI modified biochar

At present, common methods of loading iron species can be divided into two major categories illustrated in Fig. 2, which are: (1) pre-treatment: iron salts or iron metal oxides are mixed with biomass raw materials and then co-pyrolyzed to obtain iron-based biochar catalysts, which can be called impregnation pyrolysis; (2) post-treatment includes co-precipitation, and reductive co-deposition. Impregnation pyrolysis is simple and easy to future scale-produce, but the size and morphology of iron particles tend to be out of control, while post-treatment can better regulate the morphology of iron particles, such as nanoparticle size and ferric valence.

Zero-valent iron has significant catalysis performance on persulfate, but nanoparticle ZVI tends to agglomerate due to its large surface energy and electric adsorption. Also, nano-ZVI is easily oxidized and has poor dispersibility, limiting its further application. Loading ZVI on biochar can help to overcome the above problems [52,53].

The loading methods commonly include ball milling, liquid phase reduction, thermal decomposition, hydrothermal method. Among these methods, the liquid phase reduction method is the most efficient and common. Biochar is directly added to the iron salt solution and the reducing agent is commonly used as sodium borohydride. Wang *et al.* directly used iron-containing sludge from municipal wastewater treatment plants directly reduced to ZVI by the addition of $NaBH_4$ [54]. This method can be finished without an extra iron addition. The degradation efficiency of AO7 increased from 59.9% to 99.0%. The degradation efficiency was 7 times higher than that of unmodified biochar, which provided a great idea for the disposal of phosphorus removal sludge.

The introduction of biochar as the carrier for ZVI can effectively alleviate easy agglomeration of nano-ZVI [55]. But the biochar carrier has a low interaction force between iron species, facing easy oxidation of ZVI [56]. Wu *et al.* wrapped nano nano-ZVI particles in iron oxide (Fe_2O_3·FeO) and graphite layers by citrate chelation-assisted co-assembly and carbon thermal reduction [57]. And ZVI was uniformly dispersed in mesoporous carbon so that the wrapped ZVI-biochar catalysts were stable in air for 20 days without oxidation. Also, the wrapped ZVI-biochar catalysts showed low iron leaching, at only 1.5 mg/L.

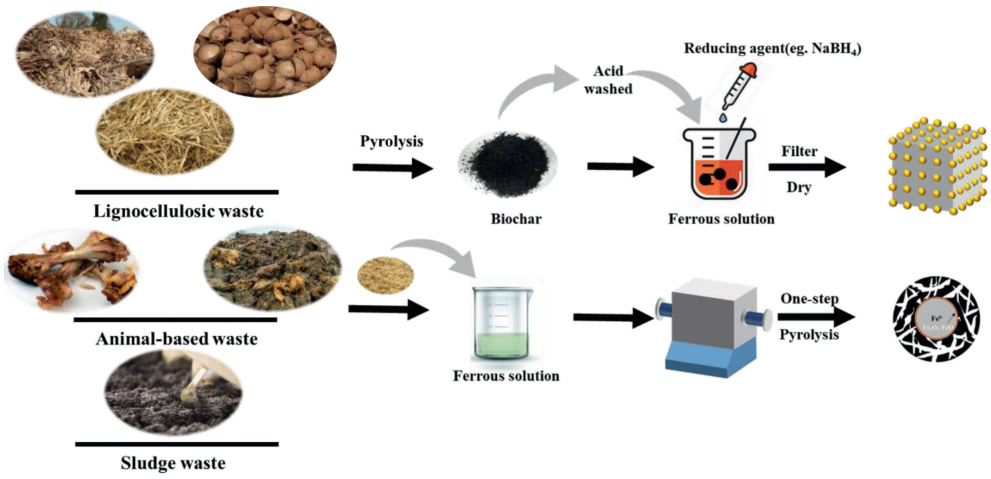

Fig. 2. Two main preparation methods of ZVI-modified biochar.

In addition to introducing reducing reagents, ZVI can also be directly obtained during the pyrolysis process. Jiang *et al.* prepared ZVI-BC by pyrolyzed iron pretreatment biomass in N_2 environment [58]. And the results showed that the valence state of iron was gradually converted from high to zero valence with the increase of pyrolysis temperature and residence time. This is due to the release of reductive gaseous products such as H_2, and CO evolving from the thermal decomposition of biomass during high-temperature pyrolysis. And similar direct reduction phenomenon was also observed in the study of Wang *et al.* [59]. The prepared Fe-rich biochar prepared at 500 °C pyrolysis temperature was mainly in the form of Fe_2O_3. With the increase of temperature to 700 °C, Fe_2O_3 was reduced to FeO, and with the further increase of temperature to 900 °C, all iron species were reduced to ZVI.

In this section, ZVI-loaded biochar revealed excellent catalysis performance and better resistance to oxidation and agglomeration. During the catalysis process, ZVI can also help Fe^{3+} reduce to Fe^{2+}, which can prolong the catalysts lifetime.

3.2. Iron oxide modified biochar

Iron oxides (Fe_2O_3 and Fe_3O_4) are the most common catalysts used to activate persulfate for the degradation of emerging pollutants. And their catalytic performance has been widely studied and recognized [52,60]. Among them, Fe_3O_4 is often applied to activate persulfate as a mixed-valence oxide with the proportion of Fe(II) and Fe(III) between about 0.30 and 0.43.

Simply mixing biochar with iron oxides can not enhance catalytic performance, it may cause iron oxides to clog in biochar pores. Similar to ZVI-loaded biochar, iron oxide loaded biochar can also weaker the agglomeration of iron oxides, which will increase the exposure of active sites to enhance the degradation efficiency. Cui *et al.* directly precipitated Fe_3O_4 on biochar by a one-step method to synthesize Fe_3O_4-biochar [61]. The degradation of BPA is a synergistic process of catalysis and adsorption, and both homogeneous and heterogeneous reactions occur simultaneously in the catalytic process. Fu *et al.* synthesized Fe_3O_4/BC by ball-milling biochar with K_2FeO_4 to obtain highly graphitized biochar [62]. They found that higher graphitization can promote direct electron transfer between HBA and PMS on the catalyst surface. Song *et al.* prepared BC-FeO_x composites for the degradation of naphthenic acid (ACA) [41]. The results showed that the removal efficiency of BC-FeO_x, FeO_x, and BC is about 96.1%, 60%, and 10%, respectively, which showed the iron-based biochar catalysts significantly enhanced the activation performance.

To further reduce the cost and environmental impact, Wang *et al.* proposed to use iron-rich waste as a raw material to reduce the cost [63]. They co-pyrolyzed iron-containing sludge with aluminum-containing red mud to prepare biochar without the external additional iron reagent to achieve 'Using waste to treat waste'. However, the specific surface area of biochar obtained from sludge pyrolysis was only 58.20 m^2/g, which was related to the high ash content in the sludge biochar [64]. The carbon content of lignocellulosic biochar is 35%-85%, while carbon content of sludge biochar is usually below 30% [58]. Therefore, there is a big difference between sludge biochar and lignocellulosic biochar. It can be attributed to the high ash content clogging some pores, resulting in low specific surface area. Hence researchers can explore how to combine sludge and lignocellulose-based biochar in a suitable way to make it have both carbon skeleton dispersion and iron-based loading [42,65]. Cho *et al.* combined lignin biomass with red mud by co-pyrolysis, the removal efficiency of MB and pCBP is 97.7% ± 0.1%, and 16.3% ± 5.8%, respectively [42]. While most removal capacity is attributed to adsorption, the catalytic performance still needs further improvement.

Except for the introduction of an exogenous iron source, Wang *et al.* studied the effect of endogenous metals of biochar [59]. They found that Fe, Mn, and Zn existed in different crystal forms after pyrolysis. Fe was in the low-valent form, Mn was in the high-valent form of $CaMnO_3$, MnS, and Zn was gradually volatilized after reduction. and it was found that Fe-rich or Zn-rich biochar showed excellent catalytic performance. In contrast, Mn-rich biochar had poor catalytic activity. This finding provides a solution for the treatment of biomass enriching in the metal element.

In this section, facile iron modification methods were provided. The introduction of iron-loaded can help improve the catalysis performance, since it may provide new active sites for persulfate activation. Also, iron-loaded pretreatment can tailor biochar structure to improve the graphitization and enlarge the specific surface area, facilitating the electron transfer and diffusion of active substances.

3.3. Heteroatom doped biochar catalysts

Doping with heteroatoms is another common modification method to enhance active sites of biochar [66]. Nitrogen atoms, due to their atomic diameter close to carbon atoms, can easily substitute sp^2-hybridized carbon atom into biochar carbon frameworks, while sulfur atoms mainly enter the biochar by replacing surface oxygen-containing functional groups. Heteroatom doping, especially nitrogen doping, was proven to be a simple but effective way to tailor the charge distribution of adjacent carbons due to its higher electronegativity ($\chi_N = 3.04$ *vs.* $\chi_C = 2.55$), which can help increase the adsorption of persulfate ions (Fig. S2 in Supporting information).

Nitrogen-doped biochar is mostly synthesized by the one-pot method, which often uses urea, melamine, and dicyandiamide as nitrogen sources, and this method is hard to control the type of nitrogen. Nitrogen doping was found to exist in the form of pyrrole nitrogen, pyridine nitrogen, and graphite nitrogen. Different nitrogen forms will bring diverse active sites by DFT calculation. Wang *et al.* found a linear relationship between the addition of pyrrole nitrogen and pyridine nitrogen and the removal efficiency [67]. For different structures of nitrogen, Duan *et al.* showed that the catalytic effect of graphite and pyridine nitrogen was much greater than that of pyrrole nitrogen [68]. Till now the different contribution of the three forms of nitrogen is still controversial. Even so, nitrogen doping is a considerable modification method for persulfate activation.

Biochar relying on nitrogen doping alone to enhance active properties has been well studied, but Fe/N co-doping is very interesting for catalysis enhancement compared to sole nitrogen doping. Xi *et al.* prepared Fe/N co-doped biochar by mixing iron salts and urea [69]. And he found the degradation process has both free radical pathways and non-free radicals, with 49.7% and 42.4% for $^{\bullet}OH$ and $^1O_2$, respectively. The $^{\bullet}OH$ was considered generated by iron sites while $^1O_2$ was attributed to C=N and graphitic nitrogen. Not only iron and nitrogen co-doped biochar can regulate the original charge density of the biochar, but also the introduction of nitrogen can work as an anchor for iron crystal growth. A similar phenomenon was confirmed in Huang's research [70]. They found that after nitrogen doping, the nitrogen site preferentially becomes an adsorption site for Fe^{2+}, thus the following growth of ZVI may more likely act at this site.

In addition to the common nitrogen doping, sulfur can also be used as a heteroatom doping to change the structure of carbon materials, primarily using thiourea as a sulfur-containing chemical reagent. Wang *et al.* found that sulfur doping can produce more Lewis acid sites, and Lewis base sites [71]. The activation of PMS tends to occur at Lewis acid sites and ROS is dominated by $^1O_2$. In contrast, the activation of PDS tends to occur at Lewis base sites and BPA may be oxidized by biochar-PDS complex.

In conclusion, heteroatom-dope biochar will achieve excellent catalysis performance. At the same time, heteroatom doping has a synergy effect with iron species to manipulate electron density on carbon frameworks.

4. Mechanism of persulfate activation by biochar-based catalysts

Diverse modification methods will enhance the catalysis performance. But the mechanisms of emerging pollutants degradation may have a big difference [72,73]. The main mechanisms of persulfate activation can be classified as free radical pathway, singlet oxygen, and direct electron transfer in Fig. S3 (Supporting information). In this section, several conclusions are introduced for mechanism discussion.

4.1. Radical mechanism

To pristine biochar, there are abundant oxygen-containing functional groups on the surface of biochar. And -OH and -COOH are generally considered to be the active sites of $SO_4^{\bullet-}$ and $^{\bullet}OH$. Researchers examined the content changes of functional groups of biochar materials before and after use by XPS, and thus hypothesized that -OH and -COOH are active sites. For most iron-loaded biochar, the modification may bring active site to produce free radicals similar to pristine biochar. But the abundance of active sites compared to pristine biochar is not at the same order magnitude, which can bring higher degradation efficiency than pristine biochar. What is more, biochar can facilitate the recycling between Fe^{3+} and Fe^{2+} by electron transfer from biochar to iron species. In the Fenton-like field, researchers mainly introduced electron-rich external structures to facilitate the reduction from Fe^{3+} to Fe^{2+}. The common electron-rich materials are carbon materials (*i.e.*, graphene carbon nanotubes, biochar), reducing or chelating agents (*i.e.*, citrate, L-cysteine [74], hydroxylamine [75]) and metal sulfides (*i.e.*, MoS_2, CoS_2, WS_2 [76,77]). Carbonaceous usually have a certain reducing ability, which could directly donate electrons to reduce Fe^{3+} [78]. Biochar compared to expensive graphene and carbon nanotubes is abundant raw material that facilitates iron recycling. In the past, it is generally believed in the homogeneous catalytic process that Fe^{2+} can be obtained by the reduction of HSO_5^- [79]. The above reaction is thermodynamically difficult to happen due to $Fe^{3+}/Fe^{2+} = 0.77$ V and $HSO_5^-/SO_5^{\bullet-} = 1.1$ V. While Fu *et al.* [62] found that the more favorable process for Fe^{3+} reduction is $O_2^{\bullet-}$ ($O_2^{\bullet-}/O_2 = -0.33$ V) by iron-based biochar catalysts and the suitable redox potential makes it easier for the reduction reaction to take place thermodynamically (Fig. S4 in Supporting information).

Also, the recycling of Fe^{3+}/Fe^{2+} can be accelerated by PFRs on the surface of biochar. This phenomenon was confirmed in the study of Liang *et al.* [80]. The promotion of low-temperature biochar has a continuous effect on the reduction of Fe^{3+}, and the conversion between semi-quinone radicals and quinones on the char surface results in the excellent reusability and continuous SMX degradation of BC400, while BC700 has difficulty in maintaining the Fe^{3+}/Fe^{3+} cycle due to the destruction of PFRs and the formation of sp^2-hybridized carbon frameworks at high pyrolysis temperature. And interestingly the main mechanism of BC700 system is direct electron transfer due to sp^2-hybridized carbon frameworks (Fig. 3a).

The abundance of Cl^- in the actual aqueous environment is often considered as a radical trapping agent, generating chlorine radicals with weak oxidative capacity and therefore decreasing the pollutant degradation efficiency. In fact, halide ions (X^-, *e.g.* Cl^-, Br^-, and I^-) can not only react with free radicals but also produce direct consumption of PMS producing halides (HOX, X_2, and OX^-) [81]. To avoid such by-products, biochar composite should test the ability to resist halide ions and natural organic matter.

Therefore, biochar and loaded iron metal have synergistic effects in the persulfate activation system. Biochar as a carrier can avoid the accumulation and aggregation of iron particles. Secondly, the adsorption and enrichment of pollutants by biochar is beneficial to the contact between active sites and pollutants, and finally, biochar can help recycle between Fe^{3+} and Fe^{2+} due to PFRs. The activation pathway of the iron-based biochar catalysts is mainly by the free radical pathway, which favors the generation of $SO_4^{\bullet-}$ and $^{\bullet}OH$ to achieve high efficiency of pollutant removal.

4.2. Singlet oxygen

The free radicals $^{\bullet}OH$ and $^{\bullet}SO_4^-$ with strong oxidizing properties are less effective in degrading pollutants in an actual aqueous environment due to unnecessary scavenged by natural organic matter (NOM) and inorganic anions. $^1O_2$ is considered to have better resistance to NOM, Cl^-, HCO_3^-, *etc.*

It is widely believed that $^1O_2$ can be generated by PMS self-decomposition, but the generation efficiency is not high. In a homogeneous system, benzoquinone has a strong activation ability under alkaline conditions to form $^1O_2$ [82]. Researchers further studied in depth to determine that C=O on the surface of biochar is also an important active site to produce $^1O_2$ (Fig. 3b). They found that the carbonyl content has a linear relationship with the catalytic activity ($R^2 = 0.971$), and the catalytic process is described in the following equation [59,83].

In the case of biochar, the C=O structure can be promoted by the passage of reducing gases such as H_2 or N_2H_4 during the pyrolysis process, while in the case of Fe-based loaded biochar, the passage of reducing gases can synergistically reduce the valence state of Fe element and promote the production of ZVI. Huang *et al.* found that the degradation efficiency of BPA was increased by 20%

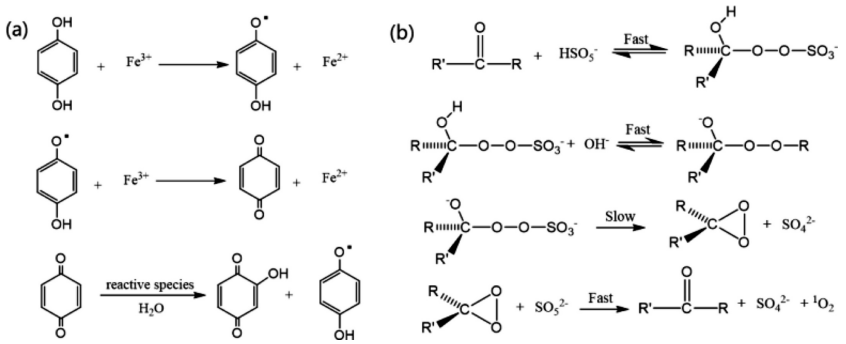

Fig. 3. (a) Reaction mechanisms of low-temperature biochar accelerating the Fe^{3+}/Fe^{2+} circulation, and (b) ketone-catalyzed PMS decomposition process.

for biochar after H_2 reduction compared to the original biochar, and in contrast, the degradation efficiency decreased to 45% after treatment with strong oxidizing acids such as HNO_3, indicating that C=O on biochar is the key active site for catalytic PMS decomposition [83].

4.3. Electron transfer

Compared with the radical-dominated advanced oxidation process, the mediated electron transfer process has higher selective oxidation and can largely avoid the adverse effects of common substrates in the water column. It is mainly through the formation of BC surface-limited activated PS complex (BC-PS*), forming an electron shuttle system, which has a high redox potential, and when there is no pollutant, slow electron transfer occurs, and when pollutants exist in the system, the electron transfer between biochar and persulfate will occur rapidly to achieve efficient degradation of pollutants.

For mono iron oxide, the poor electron conductivity hinders electron-transfer pathway. A common strategy is to integrate iron oxide onto highly conductive biochar substrate *via* sp^2-hybridized carbon frameworks [84]. Researchers nowadays mostly evaluate the electron pathway by combining electrochemical impedance spectroscopy with linear cyclic voltammetry. Usually, researchers depend on electrochemical impedance spectroscopy (EIS) to detect the conductivity of the catalysts. Higher conductivity promises to bring faster electron transfer. Furthermore, the chronoamperometry test will be direct evidence to prove electron transfer. Also, researchers will combine linear sweep voltammetry (LSV) with the above procedures. The increased current density indicates metastable reactive complex formed due to the interaction between persulfate and organic pollutants.

Ding *et al.* found that the embedded nitrogen atoms attracted electrons from adjacent carbon atoms due to the electronegativity difference resulting [85]. It can help form positively charged carbon, facilitating the adsorption of HSO_5^-. Here, PMS received two electrons from pollutants and was decomposed into SO_4^{2-} and OH^-, accelerating the degradation of the pollutant. Wang *et al.* similarly found N-doped biochar changed the dominant mechanism from singlet oxygen to electron transfer, in which edge nitrogen configuration may be the critical reactive site [67].

Iron-based biochar catalysts under high-temperature pyrolysis also contributed to mediating the electron transfer pathway. Liang *et al.* developed iron-based biochar catalysts *via* high-temperature pyrolysis (BC/Fe-700). They found that surface-mediated electron transfer dominated the oxidation process [86]. In real water matrixes, the composite exhibits the great superiority of the electron transfer system. However, the relations of treatment temperature, property of composites, and regime of oxidation are still unclear. Hence, more studies are required to fully understand the novel oxidation technology based on the nonradical activation of persulfate.

5. Theoretical calculation for mechanisms interpretation

The improvement of catalysis performance by iron-loaded biochar has been widely proven. But the certain role of biochar and iron species is still unclear. The interaction between biochar and iron species deserves future attention. Biochar is commonly used as substrates to host iron clusters since they provide anchoring sites (*e.g.*, surface defects, and vacancies). Now, Huang *et al.* found after nitrogen doping, the nitrogen site preferentially becomes an anchoring site for Fe^{2+}, and nanoparticles of ZVI tend to grow at this site [70]. Also, introducing iron species to biochar may regulate the electron density of carbon layer. Gao *et al.* [87] induced iron materials to biochar and the concertation of sp^2-hybridized carbon increased from 73.28% to 84.65%. The sp^2-hybridized carbon frameworks bring better performance for adsorption and electron transfer than sp^3-hybridized and amorphous carbon frameworks.

Theoretical calculation based on DFT is a powerful tool to prove the possible reaction mechanism of biochar-based SR-AOPs and active sites. Iron doping tuned the activation barrier and pathway toward persulfate activation [88]. By density functional theory (DFT), researchers can interpret different mechanisms. Li [89] prepared the single-atom iron biochar material (ISA-Fe/MC) in form of Fe-N_x-C structure obtained after acid etching of the nano-Fe biochar material (Nano-Fe/MC). And the former is an electron transfer-dominated reaction process while the latter is a radical-dominated reaction process for the two materials with the same substrate. After DFT calculations, it was found that strong charge accumulation and low electron transfer resistance existed between monatomic Fe and graphitized carbon layers to achieve the coupling effect between monatomic Fe and graphitized carbon layers, and Fe-C bonding was considered as a bridge for electron transfer; whereas this phenomenon did not exist in Nano-Fe/MC, leading to a radical-dominated activation process. Nowadays, DFT calculations are mostly used to optimize the structure of PMS molecules with the material surface by calculating the adsorption energy (E_{ads}), O-O length ($l_{O\text{-}O}$) and electron transfer number (Q) in combination with experimental phenomena to infer the activation mechanism. The calculation process found it has lower adsorption energy (−6.07 eV) and longer $l_{O\text{-}O}$ (1.47 Å), accompanied by strong electron transfer, corroborating that the NMB surface has strong active sites for adsorption of PMS activation to produce $^{\bullet}OH$, $SO_4^{\bullet-}$ radicals [90] (Fig. S5 in Supporting information). Iron doping could alter the activation mode for PMS, resulting in an increased number of electron transmissions for improved breakage of O-O bond in PMS. Such a synergistic effect optimized the electronic density and configuration, which significantly suppressed metal ion leaching and accelerated the catalytic process and catalytic stability (Table S2 in Supporting information). In the future, the more accurate judgment of reactive sites and mechanism still need to be deeply and systematically investigated. Better catalyst configuration can be created by a deeper understanding of the synergistic relationship between iron species and biochar.

6. Reusability and regeneration of biochar catalysts

During the SR-AOPs process not only does biochar act as a catalyst to stimulate ROS, but also biochar itself will be attacked by ROS, which may affect the biochar-based catalyst's recycling. In other words, catalyst's high recycling and reuse are vital for economic efficiency in the wastewater treatment process.

Reusability and stability are vital for catalysts used in pollutant degradation. The long-term catalytic efficiency of biochar catalysts also needs to be evaluated for further field-scale application [91]. Zhang *et al.* found after the fourth cycle tests the catalytic ability of BC began to decrease, likely due to catalyst deactivation *via* the deposition of small molecular contaminants onto its surface [92]. And for iron-based biochar, the concertation of iron leaching is an important parameter. Xin *et al.* tested the concertation of leached ions is below 0.02 mg/L after 300 min reaction at pH 5.0, which is significantly below discharge limits [93].

Due to the decreased efficiency of the reusability test, regeneration methods are also required. Usually, the regeneration methods can be classified into two categories, referred to here as thermal and solvent regeneration. Sun *et al.* by partial oxidation restored catalytic activity of biochar [94]. After 0.4% oxygen was introduced for 7 min, the external surface area and the microporous area of biochar increased significantly from 574 m^2/g to 939 m^2/g. Liu *et al.* washed biochar with ethanol and pyrolysis at 500 °C [95]. After ethanol washing, the removal of 2,4-DCP was revered from 50% to 70%. And after pyrolysis at 500 °C, the removal rate increased to

80%. The characteristic of thermal regeneration is high efficiency but large energy consumption. At the same time, solvent regeneration may cause secondary pollution.

7. Conclusion and prospects

This review concludes recent year research progress of biochar-activated persulfate degrading emerging pollutants, especially focusing on iron-based biochar catalysts. In conclusion, the basic characteristics of the element component, specific surface area, and pore type are directly affected by biomass feedstock, pyrolysis condition, and pretreatment methods. The pristine biochar has still limited catalytic efficiency, while iron modification can bring more active sites. Using iron-based biochar catalysts for persulfate activation indeed overcomes the disadvantages of the mono use of either BC or iron nanoparticles. Iron modification of biochar catalysts can adjust effectively the pore structure, surface functions, and interactions between iron particles and biochar. Iron doping enhances surface area in line with the pore of biochar, while biochar provided an anchor for iron nanoparticles to overcome the agglomeration. Also, iron-based biochar driving persulfate activation may change the activation mechanism from radical dominant to electron transfer, such as Fe-N_x-C structure or high-temperature pyrolysis. Through iron modification, the metal wrapped in the carbon matrix can improve the catalyst's electron transfer efficiency and serve as additional redox catalytic sites. By DFT calculation, charge density analysis can demonstrate the significant electron transfer between persulfate and biochar catalysts.

Future research and perspectives are described below according to current understanding.

(1) Green and facile preparation methods are required for biochar catalysts. Green preparation process focused on two aspects, one is to reduce organic solvents used in the catalyst preparation process, the other is to establish energy-saving routes to mediate the surface properties and catalysis performance for efficient contaminant removal. Current preparation and synthesis of biochar materials focus more on their environmental remediation performance, such as catalytic ability and adsorption capacity. While, they still lack systematic consideration of the greenness, yield, and economy of their preparation process. For example, using iron-containing sludge or biomass enriching in metal element is a solution to decrease the preparation cost, avoiding the consumption of chemicals produced by external iron sources. Future researchers should evaluate the environmental fate of biochar catalysts, and their potential impacts on the ecosystem over time.

(2) The practical application of biochar activation persulfate deserves more attempts. Current research mainly focuses on batch-scale experiments, and the concentration of simulated emerging pollutants is often higher than actual circumstances. Actually, not only can biochar-activation persulfate apply to remove emerging contaminants in municipal wastewater treatment and industrial wastewater treatment, but also it can apply to groundwater remediation such as permeable reaction barrier and *in-situ* chemical oxidation. More pilot-scale and field-scale applications are required to evaluate the performance of biochar catalysts in the real environment.

(3) The activation mechanisms still need to explore with combined of more acute models. According to the current quenching experiment, EPR tests, and DFT calculation, the basic activation mechanisms have been explored. But due to the complexity of biochar, the structure-function relationship is still hard to conclude. In the future, researchers could combine machine learning with traditional environment models to further explore the activation mechanisms. Another way is to synthesize similar property polymers to simulate the key property of biochar.

(4) Life cycle analysis for biochar catalysts is important for future application. Biochar materials have been extensively studied as catalyst activation effects, and how to dispose of waste biochar catalysts will be a hot issue in the future. Biochar itself has good biocompatibility, and how to realize the harmlessness and simplicity of waste catalysts dispose is important for future research work.

Declaration of competing interest

The authors declare that they have no known competing financial interests or personal relationships that would appear to influence the work reported in this paper.

Acknowledgment

This work was supported by the National Natural Science Foundation of China (No. 51778230).

Supplementary materials

Supplementary material associated with this article can be found, in the online version, at doi:10.1016/j.cclet.2023.108357.

References

[1] Y.L. Luo, W.S. Guo, H.H. Ngo, et al., Sci. Total Environ. 473 (2014) 619–641.
[2] Y. He, M. Gao, Y. Zhou, Y. Zhou, Chemosphere 311 (2023) 136925.
[3] T. Wang, J. He, J. Lu, et al., Chin. Chem. Lett. 33 (2021) 3585–3593.
[4] X. Chen, M.F. Hossain, C. Duan, et al., Chemosphere 307 (2022) 135545.
[5] C. Duan, J. Wang, Q. Liu, et al., Sep. Purif. Technol. 282 (2022) 120013.
[6] H. Qiu, W. Ni, L. Yang, Q. Zhang, Chem. Eng. J. 450 (2022) 138161.
[7] T. Deblonde, C.L. Carole, P. Hartemann, Int. J. Hyg. Environ. Health 214 (2011) 442–448.
[8] Q. Zhou, Z. Yue, Q. Li, et al., Environ. Sci. Technol. 53 (2019) 13408–13416.
[9] Q. Liu, J. Wang, C. Duan, et al., J. Hazard. Mater. 426 (2022) 128074.
[10] M. Xu, X. Gu, S. Lu, et al., Front. Environ. Sci. Eng. 10 (2016) 438–446.
[11] F. Ghanbari, M. Moradi, Chem. Eng. J. 310 (2017) 41–62.
[12] J. Wang, S. Wang, Chem. Eng. J. 334 (2018) 1502–1517.
[13] S. Yang, P. Wang, X. Yang, et al., J. Hazard. Mater. 179 (2010) 552–558.
[14] Q. Luo, Front. Environ. Sci. Eng. 8 (2014) 188–194.
[15] S.H. Do, J.H. Jo, Y.H. Jo, et al., Chemosphere 77 (2009) 1127–1131.
[16] J. Zou, J. Ma, L. Chen, et al., Environ. Sci. Technol. 47 (2013) 11685–11691.
[17] J. Du, J. Bao, Y. Liu, et al., J. Hazard. Mater. 320 (2016) 150–159.
[18] H. Sun, S. Liu, G. Zhou, et al., ACS Appl. Mater. Interfaces 4 (2012) 5466–5471.
[19] H. Liu, P. Sun, M. Feng, et al., Appl. Catal. B 187 (2016) 1–10.
[20] B. Liu, W. Song, H. Wu, et al., Chem. Eng. J. 398 (2020) 125498.
[21] X. Du, S. Wang, F. Ye, Q. Zhang, Environ. Res. 206 (2022) 112414.
[22] G.P. Anipsitakis, D.D. Dionysiou, Environ. Sci. Technol. 38 (2004) 3705–3712.
[23] Y. Zhou, J. Lu, Y. Zhou, Y. Liu, Environ. Pollut. 252 (2019) 352–365.
[24] C. Duan, T. Ma, J. Wang, Y. Zhou, J. Water Process Eng. 37 (2020) 101339.
[25] Y. Song, X. Song, Q. Sun, et al., Sci. Total Environ. 803 (2022) 150087.
[26] J. Zhang, X. Shao, C. Shi, S. Yang, Chem. Eng. J. 232 (2013) 259–265.
[27] X. Duan, H. Sun, S. Wang, Acc. Chem. Res. 51 (2018) 678–687.
[28] H. Lee, H. Lee, J. Jeong, et al., Chem. Eng. J. 266 (2015) 28–33.
[29] C. Wang, J. Kang, P. Liang, et al., Environ. Sci. Nano 4 (2017) 170–179.
[30] X. Zhang, Y. Wang, N. Ju, et al., ACS Sustainable Chem. Eng. 9 (2021) 8813–8823.
[31] X.J. Lee, H.C. Ong, Y.Y. Gan, et al., Energy Convers. Manage. 210 (2020) 112707.
[32] Y.D. Chen, F. Liu, N.Q. Ren, S.H. Ho, Chin. Chem. Lett. 31 (2020) 2591–2602.
[33] H.W. Lee, H. Lee, Y.M. Kim, et al., Chin. Chem. Lett. 30 (2019) 2147–2150.
[34] X. Li, Y. Jia, J. Zhang, et al., Chin. Chem. Lett. 33 (2022) 2105–2110.
[35] S. Nimai, H. Zhang, Z. Wu, et al., Chin. Chem. Lett. 31 (2020) 2657–2660.
[36] G. Song, F.Z. Qin, J.F. Yu, et al., J. Hazard. Mater. 424 (2022) 127663.
[37] X. Li, T. Hao, Y. Tang, G. Chen, Front. Environ. Sci. Eng. 15 (2020) 3.
[38] K. Tian, L. Hu, L. Li, et al., Chin. Chem. Lett. 33 (2022) 4461–4477.
[39] W.J. Liu, H. Jiang, H.Q. Yu, Chem. Rev. 115 (2015) 12251–12285.
[40] Y.Q. Sun, I.K.M. Yu, D.C.W. Tsang, et al., Chem. Eng. J. 398 (2020) 125505.
[41] J. Song, Z.T. How, Z. Huang, Chem. Eng. J. 429 (2022) 132220.
[42] D.W. Cho, K. Yoon, Y. Ahn, et al., J. Hazard. Mater. 374 (2019) 412–419.
[43] S. Xia, K. Li, H. Xiao, et al., Bioresour. Technol. 287 (2019) 121444.
[44] K.J. Nakarmi, E. Daneshvar, G. Eshaq, et al., Environ. Res. 214 (2022) 114041.
[45] A.A. Ioannidi, J. Vakros, Z. Frontistis, D. Mantzavinos, Catalysts 12 (2022) 1245.

[46] X. Ruan, Y. Sun, W. Du, et al., Bioresour. Technol. 281 (2019) 457–468.
[47] H. Han, W. Buss, Y. Zheng, et al., Chem. Eng. J. 429 (2022) 132287.
[48] G. Fang, C. Liu, J. Gao, et al., Environ. Sci. Technol. 49 (2015) 5645–5653.
[49] G. Fang, J. Gao, C. Liu, et al., Environ. Sci. Technol. 48 (2014) 1902–1910.
[50] X.X. Ruan, Y.Y. Liu, G.Q. Wang, et al., Bioresour. Technol. 270 (2018) 223–229.
[51] K. Talukdar, B.M. Jun, Y. Yoon, et al., J. Hazard. Mater. 398 (2020) 123025.
[52] L. Ling, J. Lu, Y. Zhou, Y. Zhou, Res. Environ. Sci. 35 (2022) 290–298.
[53] Y. He, Y. Zhou, J. Feng, M. Xing, Environ. Func. Mater. 1 (2022) 204–217.
[54] J. Wang, M. Shen, Q. Gong, et al., Sci. Total Environ. 714 (2020) 136728.
[55] Z. Ma, H. Cao, F. Lv, et al., Front. Environ. Sci. Eng. 15 (2021) 98.
[56] Y.H. Lin, H.H. Tseng, M.Y. Wey, M.D. Lin, Sci. Total Environ. 408 (2010) 2260–2267.
[57] Y. Wu, X. Chen, Y. Han, et al., Environ. Sci. Technol. 53 (2019) 9081–9090.
[58] S.F. Jiang, L.L. Ling, W.J. Chen, et al., Chem. Eng. J. 359 (2019) 572–583.
[59] X. Wang, P. Zhang, C. Wang, et al., J. Hazard. Mater. 424 (2022) 127225.
[60] F. Ji, C. Li, X. Wei, J. Yu, Chem. Eng. J. 231 (2013) 434–440.
[61] X.W. Cui, S.S. Zhang, Y. Geng, et al., Sep. Purif. Technol. 276 (2021) 119351.
[62] H. Fu, P. Zhao, S. Xu, et al., Chem. Eng. J. 375 (2019) 121980.
[63] J. Wang, M. Shen, H. Wang, et al., Sci. Total Environ. 740 (2020) 140388.
[64] H. Wang, J. Xu, L. Sheng, J. Cleaner Prod. 273 (2020) 123131.
[65] Y. Du, M. Dai, J. Cao, C.J.R.a. Peng, RSC Adv. 9 (2019) 33486–33496.
[66] K. Pang, W. Sun, F. Ye, et al., J. Hazard. Mater. 424 (2022) 127270.
[67] H. Wang, W. Guo, B. Liu, et al., Water Res. 160 (2019) 405–414.
[68] X. Duan, H. Sun, Y. Wang, et al., ACS Catal. 5 (2015) 553–559.
[69] M. Xi, K. Cui, M. Cui, et al., Chem. Eng. J. 420 (2021) 129902.
[70] P. Huang, P. Zhang, C. Wang, et al., Appl. Catal. B 303 (2022) 120926.
[71] H. Wang, W. Guo, B. Liu, et al., Appl. Catal. B 279 (2020) 119361.
[72] J. Huang, H. Zhang, Front. Environ. Sci. Eng. 13 (2019) 65.
[73] X. Liu, X. Su, S. Tian, et al., Front. Environ. Sci. Eng. 15 (2020) 75.
[74] J. Lu, T. Wang, Y. Zhou, et al., J. Hazard. Mater. 383 (2020) 121133.
[75] L. Li, S. Liu, M. Cheng, et al., J. Hazard. Mater. 406 (2021) 124333.
[76] J. Lu, Y. Zhou, J. Lei, et al., Chemosphere 251 (2020) 126402.
[77] J. Lu, Y. Zhou, L. Ling, Y. Zhou, Chem. Eng. J. 446 (2022) 137067.
[78] H. Ding, Y. Zhu, Y. Wu, et al., Environ. Sci. Technol. 54 (2020) 10944–10953.
[79] W.D. Oh, Z. Dong, T.T. Lim, Appl. Catal. B 194 (2016) 169–201.
[80] J. Liang, X. Duan, X. Xu, et al., Appl. Catal. B 297 (2021) 120446.
[81] W. Peng, Y. Dong, Y. Fu, et al., Chem. Eng. J. 421 (2021) 127818.
[82] Y. Zhou, J. Jiang, Y. Gao, et al., Environ. Sci. Technol. 49 (2015) 12941–12950.
[83] B.C. Huang, J. Jiang, G.X. Huang, H.Q. Yu, J. Mater. Chem. A 6 (2018) 8978–8985.
[84] S.M. Shaheen, A. Mosa, Natasha, et al., Biochar 4 (2022) 24.
[85] D. Ding, S. Yang, X. Qian, et al., Appl. Catal. B 263 (2020) 118348.
[86] J. Liang, X. Duan, X. Xu, et al., Environ. Sci. Technol. 55 (2021) 10077–10086.
[87] L. Guo, L. Zhao, Y. Tang, et al., Chem. Eng. J. 435 (2022) 135189.
[88] B. Zhang, X. Li, P.A. Bingham, et al., Chem. Eng. J. 451 (2023) 138574.
[89] Z. Li, K. Li, S. Ma, et al., J. Colloid Interface Sci. 582 (2021) 598–609.
[90] J. Zhong, Y. Feng, B. Yang, et al., Sep. Purif. Technol. 289 (2022) 120735.
[91] T. Wang, J. Lu, J. Lei, et al., Sep. Purif. Technol. 307 (2023) 122755.
[92] H. Zhang, G. Xue, H. Chen, X. Li, Chemosphere 191 (2018) 64–71.
[93] S. Xin, G. Liu, X. Ma, et al., Appl. Catal. B 280 (2021) 119386.
[94] H. Sun, D. Feng, Y. Zhang, et al., Fuel 330 (2022) 125572.
[95] H. Liu, Y. Liu, L. Tang, et al., Sci. Total Environ. 745 (2020) 141095.